A MONTE CARLO STUDY OF FLEXIBLE POLYMER CHAIN CONFORMATIONS IN RESTRICTED VOLUMES. I. A MODEL FOR INSOLUBLE BLOCKS CONFORMATIONS IN SWOLLEN CORES OF MULTIMOLECULAR SPHERICAL BLOCK COPOLYMER MICELLES

Zuzana LIMPOUCHOVÁ and Karel PROCHÁZKA

Department of Physical and Macromolecular Chemistry, Charles University, 128 40 Prague 2, The Czech Republic

Received April 5, 1993
Accepted May 15, 1993

Dedicated to Professor Otto Wichterle on the occasion of his 80th birthday.

Monte Carlo simulations of chain conformations in a restricted spherical volume at relatively high densities of segments were performed for various numbers of chains, N, and chain lengths (number of segments), L, on a tetrahedral lattice. All chains are randomly end-tethered to the surface of the sphere. A relatively uniform surface density of the tethered ends is guaranteed in our simulations. A simultaneous self-avoiding walk of all chains creates starting conformations for a subsequent equilibration. A modified algorithm similar to that of Siepmann and Frenkel is used for the equilibration of the chain conformations. In this paper, only a geometrical excluded volume effect of segments is considered. Various structural and conformational characteristics, e.g. segment densities $g_S(r)$, free ends densities $g_F(r)$ as functions of the position in the sphere (a distance from the center), distributions of tethered-to-free end distances, $\rho_{TF}(r_{TF})$, etc. are calculated and their physical meaning is discussed. The model is suitable for studies of chain conformations in swollen cores of multimolecular block copolymer micelles and for interpretation of non-radiative excitation energy migration in polymeric micellar systems.

Block copolymers in dilute solutions in selective solvents (good for one block and poor for the other) self-associate forming fairly uniform multimolecular micelles, cores of which consist of insoluble blocks and shells of soluble blocks[1]. Like soap and detergent micellization in aqueous media, the copolymer micellization obeys a model of a closed association between unimer (molecularly dissolved copolymer) and micelles[2].

Micellization of block copolymers is a complex process and its thermodynamic description resulting in a reasonable prediction of equilibrium properties of micellizing systems is a difficult scientific problem. Association number, structural and thermodynamic properties of micelles depend on chemical nature, architecture and

composition of the copolymer sample, on thermodynamic quality and selectivity of the solvent and on temperature.

Gibbs free energy of the micellizing system comprises several contributions (describing behavior of the core, shell, core/shell interface, etc.), none of them being fully independent of the others. All those contributions contain inseparable entropic and enthalpic terms. Due to the above mentioned complexity of the problem, no exact and fully satisfactory theory of block copolymer micellization has been published so far. All existing theories[3-13] assume a priori that it is in principle possible to formulate separately several decisive factors controlling micellization equilibrium and to treat their effective contributions independently.

A change in the standard state chemical potential of a copolymer during the transfer from unimer into micellar state, $\Delta\mu_M^0$, is usually expressed as

$$\Delta\mu_M^0 = (\Delta\mu_M^0)_{core} + (\Delta\mu_M^0)_{shell} + (\Delta\mu_M^0)_{int} + (\Delta\mu_M^0)_{loc} . \qquad (1)$$

The first term, $(\Delta\mu_M^0)_{core}$, represents a contribution arising from the formation of a spherical micellar core from infinitely diluted insoluble blocks (recalculated to one mole of segments). This term is a sum of two contributions: (i) formation of a dense mixture of chains at the density of the core, (ii) deformation of chains due to stretching of blocks over the unperturbed dimensions. Term $(\Delta\mu_M^0)_{shell}$ is a similar contribution for the soluble blocks in the shell, $(\Delta\mu_M^0)_{int}$ corresponds to the formation of the spherical core/shell interface, and $(\Delta\mu_M^0)_{loc}$ is an entropy penalty for the location of the soluble–insoluble blocks connections in a relatively narrow interfacial region.

Due in part to the forced division of $\Delta\mu_M^0$ into several a priori defined contributions and to their simplified mathematical treatment, the full quantitative agreement of predicted and experimental data has never been reached in a broad region of solvent selectivities, temperatures and copolymer compositions. The use of approximative models for individual contributions does not allow any reliable, but speculative detailed theoretical studies of the chain behavior in various parts of a micelle. Nevertheless, the existing theories are able to explain important features of micellization equilibrium and general behavior of micellizing systems.

With the advent of powerful computers in recent years, important detailed information on molecular behavior of various polymeric systems has been obtained using Monte Carlo[14-21] and molecular dynamics computer simulations[22-25]. Computer simulations on micellizing polymer systems are at present quite rare[26-30].

Mattice et al.[26-30] simulated micellizing systems of di- and triblock copolymers in a selective solvent (precipitant for the central block of the triblock). They performed a reptation dynamics[31] combined with the Verdier algorithm[32] on a simple cubic lattice for polymer chain containing total of 20 segments. To accept a new chain con-

formation, they used the prohibition principle of the occupancy of a lattice site by two beads of a copolymer and the Metropolis rules[33]. Using interaction parameters modelling a selective solvent, the authors were able to simulate a spontaneous formation of micelles at concentrations (densities of lattice sites) higher that the critical micelle concentration without any other assumption. The aim of that study was to investigate the micellization equilibrium and some structural properties of micelles. Too short blocks of a copolymer did not allow to go into details concerning the chain arrangement in various parts of a micelle.

At present, the situation is much more convenient for advanced computer simulations of low molar mass surfactant micellizing systems[34-38]. Relatively short chains of surfactants allow simulation of a real dynamics of systems, the segments and solvent molecules of which obey the Lennard–Jones interaction potentials. Excellent simulations of Smit et al.[38] are very interesting for theoreticians from the computational point of view, but they do not offer much information as concerns polymeric micelles.

The aim of this paper is to study simultaneous arrangements of many insoluble blocks in a swollen micellar core by Monte Carlo simulations on a tetrahedral lattice. From thermodynamic point of view, our attempt is much less general and ambitious than that of Mattice et al.[26-30], or Smit et al.[38]. We start from an experimentally justified assumption that the insoluble blocks are confined in a relatively small spherical core[1]. Our simulations are therefore similar to the Monte Carlo investigations of the behavior of chains tethered to planar or curved surfaces[39-42]. In our systems, however, the chains are located inside a small spherical volume element determined by the surface.

The study is aimed to create a theoretical background necessary to explain quite unusual experimental time-resolved fluorescence and depolarization decay curves[43-45] from pendant fluorophores inside micellar cores. We suspect that the unusual decays might have been influenced by the non-radiative excitation energy migration in system of fluorophores with a non-random spatial distribution and slightly inhomogeneous microenvironments of individual fluorophores. A systematic study of chain conformations, free chain ends locations within a core, etc., should offer a distribution of fluorophores in end-tagged copolymer micelles for computer simulations of excitation energy migration (similar to those in refs[46,47]) and thus possible explanations of the time-resolved fluorimetry measurements in such systems and simultaneously should elucidate some aspects of the thermodynamics of micellization.

METHOD

A spherical cavity of a radius $R = 10\,l$ (l is the lattice sites distance) containing $S_{tot} = 2\,718$ lattice sites is located on a tetrahedral lattice. N polymer chains (each containing

L segments of the length l) tethered to the spherical surface of the cavity are randomly placed into the cavity. The first segments of all chains (i.e., the tethered ones) are placed at random into a narrow spherical surface layer of the thickness 0.1 l containing S_{int} = 99 sites. The only limitation is that none of the distances of the $N(N - 1)/2$ tethered segments pairs must be less than a certain limit, 3 l, in order to get a relatively uniform surface density of the tethered chain ends. In our calculations, N ranged from 15 to 40 and L from 20 to 90. A total number of segments, $N L$, was in the range from 400 to 1 800 which corresponded to the occupation density of the lattice sites 0.15 to 0.66. The physical nature of the problem did not required to use the periodic boundary conditions[15].

In this work, only a geometrical excluded volume effect of polymer segments was studied (single occupancy of lattice sites by one segment only) which means that no interaction parameters were considered and it simplified and accelerated significantly all simulations.

The simulations were performed as follows:

a) A simultaneous self-avoiding walk of all chains tethered to the surface was performed inside the sphere. For the self-avoiding walk, also the non-occupied lattice sites in the interfacial surface layer may be used.

b) If a local collision of several chains in the k-th step hinders the further growth of chains, one of the colliding chains is disregarded and a new chain is grown up from a new random surface site up to the k-th step. Then the procedure *a*) continues.

c) If the remedy *b*) fails several times (i.e., a generation of $3 . 10^4$ random numbers for a new non-colliding chain does not help), a random integer number $i \in \langle 1, 4 \rangle$ is generated and all chains are cut by i steps and then the growth according to *a*) continues from the $(k - i)$-th step.

d) A combination of *a*), *b*) and *c*) continues until a micellar core containing $N L$ segments is accepted.

e) As soon as a micellar core is successfully generated, one chain is chosen at random and disregarded, and a new chain is generated from a randomly selected site in the surface area in the dense medium (the whole chain is generated at the constant density of the core). This step is repeated $(N^2/2)$ times in order to remove partially the unproper bias which was caused by the fact that the average density of the core was changing during the simultaneous grows of chains.

f) To calculate segment densities, distributions of the chain free ends, etc., in an equilibrated system, a specific modification of the procedure proposed by Siepmann and Frenkel[18] for dense systems was used: The procedure *e*) is performed again $(N^2/2)$ times and the Rosenbluth weights[48], W_k, are calculated successively in all steps k (k = 1, . . ., L; W_1 = 1). A new conformation of the chain is accepted according to a modified criterion of the Metropolis type[33] – a random number RAND $\langle 0, 1 \rangle$ is generated and the new conformation is accepted if RAND $\langle 0, 1 \rangle < (W_{new}/W_{old})$, where W_{new} and W_{old} are

the weights of the whole new and old chains, respectively. The chain conformations of the last N accepted chains are taken as an equilibrated micellar core into calculations of various distributions. To generate one such micellar core, a total of (N^2L) successful generations of segment positions in a dense medium (typically $10^4 - 10^5$) is necessary.

g) All distributions were calculated on the basis of $2 \cdot 10^3$ to 10^4 generations of statistically uncorrelated and "thermally equilibrated" micellar cores. Each core was created independently, starting at the stage *a*) and finishing with *f*) which represented a simulation of approximately 10^6 chains ($10^8 - 10^9$ segment positions) altogether.

Calculations were performed partially at the PC 486 computer and partially at the DEC 5000/200 work-station. An original simulation program was created in FORTRAN77. Computations for high densities (0.6) took typically several days at PC 486 using the NDP FORTRAN compiler (they were almost 10 times faster with the DEC 5000/200). The used equilibration procedure was found to be faster and more efficient for our systems than the three-bonds "crankshaft" motion (a modification of the Verdier algorithm[32]).

RESULTS AND DISCUSSION

In order to get as much information as possible on the simulation procedure and on the behaviour of chains in a restricted spherical volume at relatively high segment densities, we have performed simulations in a broad range of chain numbers, N, and segment numbers, L.

In this communication, we present mainly results of calculations for: (i) 20 chains with the varying length, L, and (ii) constant average segment density, $\langle g_S \rangle = 0.37$, e.g. a constant product $(NL) = 1\,000$. Figure 1 depicts the segment densities, $g_S(r)$, as functions of the distance from the sphere center, r, for $N = 20$ and several chain lengths, L, (Fig. 1*a*) and for a constant number (NL) of all segments, (Fig. 1*b*). Numerical values

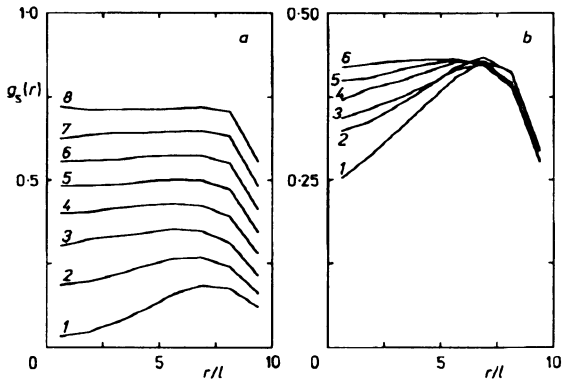

FIG. 1
Segment density, $g_S(r)$, as a function of the distance from the center of the spherical core, r/l. *a* Curves for a constant number of chains, $N = 20$, and various numbers of segments, L: *1* 20, *2* 30, *3* 40, *4* 50, *5* 60, *6* 70, *7* 80 and *8* 90; *b* Curves for a constant number of segments, $N\,L = 1\,000$ (i.e. an average density of occupated lattice sites $\langle g_S \rangle = 0.37$): $N = 40$, $L = 25$ (*1*), $N = 35$, $L = 29$ (*2*), $N = 30$, $L = 33$ (*3*), $N = 25$, $L = 40$ (*4*), $N = 20$, $L = 50$ (*5*) and $N = 15$, $L = 67$ (*6*)

of $g_S(r)$ are calculated as a fraction of the occupied-from-all lattice sites in narrow concentric spherical layers of the thickness $d = 1.25\ l$ and the inner radius $r = d\ l$. An average segment density $\langle g_S \rangle$ is: $\langle g_S \rangle = (NL)/S_{tot}$, where $S_{tot} = 2\ 718$ is the total number of the lattice sites in the sphere. Due to the decreasing numbers of the lattice sites towards the core center, the random errors in statistical computations of $g_S(r)$ increase in the central region.

Not all combinations of N and L are physically reasonable for a realistic micelle. Short chains do not reach often into the central area of the spherical core and the actual segment density, $g_S(r)$, decreases towards the core center and the micelle reminds to a certain extent a hollow sphere. This situation, which is easy to understand, is illustrated in Fig. 1*a* (curves *1* and *2*) and Fig. 1*b* (curves *1*, *2* and *3*). It is an experimentally established fact[1,49] that the segment density in realistic micellar cores is almost constant. Only in the surface region, it decreases steeply, but the decrease is partially compensated due to an intermixing with the soluble blocks (which we do not take account in our calculations). It means that the product (NL) for a realistic micellar core should guarantee a reasonably constant $g_S(r)$ in the whole sphere.

In Fig. 2, the density of chain free ends, $g_F(r)$, as a function of r is shown for the same conditions as in Fig. 1. A reliable knowledge of this distribution is extremely important for an interpretation of the excitation energy migration or fluorescence quenching experiments in micelles formed by end-tagged block copolymers[43-45]. It is evident that in systems with higher numbers of shorter chains, $(N > L)$, where the total segment density, $g_S(r)$ decreases towards the sphere center, the density of free chain ends increases considerably in this region (Fig. 2*b*). In systems with lower numbers or longer chains, $(N < L)$, variations in both $g_S(r)$ and $g_F(r)$ are less pronounced (see Fig. 2*a*), which suggest that individual chains are more coiled and more homogeneously interpenetrated. For very short chains at low segment densities, $g_F(r)$ decreases in

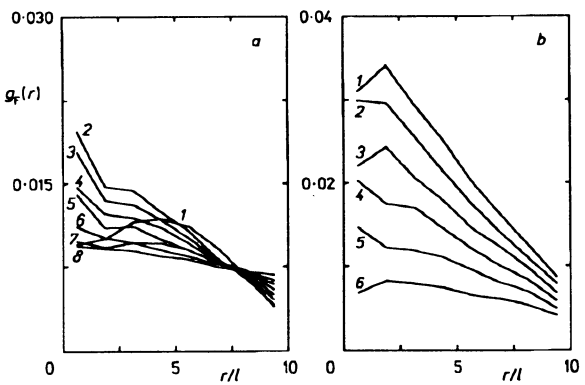

FIG. 2
Density of chain free ends, $g_F(r)$, as a function of the distance from the center of the spherical core, r/l, for the same combinations of N and L as in Fig. 1

the central region (Fig. 2*a*, curve *1*), since the behavior of a particular chain is only slightly influenced by the other chain conformations at low densities. Short chains, despite the fact that they are tethered, exhibit at low densities certain features of the behavior of an isolated free chain – geometrical constrains are more important either for long chain, or at higher densities. The values of $g_F(r)$ are on average L times lower than $g_S(r)$ as they take into account only numbers of chain ends, N, and do not depend on L, whereas functions $g_S(r)$ describe the spatial densities of (NL) segments. An average value of $\langle g_F \rangle$ is $\langle g_F \rangle = N/S_{tot}$.

Conformational behavior of individual chains in a micellar core is described by the end-to-end distribution function, $\rho_{TF}(r_{TF})$, which corresponds to the probability that the free end of the chain is located in the distance r_{TF} from the corresponding tethered end. This distribution function was calculated on the basis of N pairs of corresponding chain ends as follows: A system of concentric segmental spherical layers of the thickness d is drawn around a tethered chain end inside the core. If the corresponding free end falls into the layer with the radius $r_{TF} = i\,d$, the value $(1/S_i)$ is cumulated into the narrow slice $\Delta\rho_{TF} = \rho_{TF}(r_{TF} = i\,d) - \rho_{TF}(r_{TF} = (i-1)\,d)$, where S_i is the number of all sites in this layer. The calculated distribution is then reconstructed as an histogram for all N chains in each simulated micelle in the course of repeated computations. The principle of this calculation is schematically shown for a twodimensional rectangular lattice in Fig. 3. Absolute values of $\rho_{TF}(r_{TF})$ are small which is understandable since the space-average density of the free-to-tethered end positions for an individual chain is $(S_{tot} - 1)^{-1}$; for a chain significantly longer than $2\,R$, the free end may be a priori located in any of $(S_{tot} - 1)$ positions. In contrast to the two previous distributions, $g_S(r)$ and $g_F(r)$, which are defined for $r \in \langle 0, R \rangle$ and describe average properties of a micelle, the function $\rho_{TF}(r_{TF})$ is defined for $r_{FT} \in \langle 0, 2\,R \rangle$ and describes conformations of a single chain.

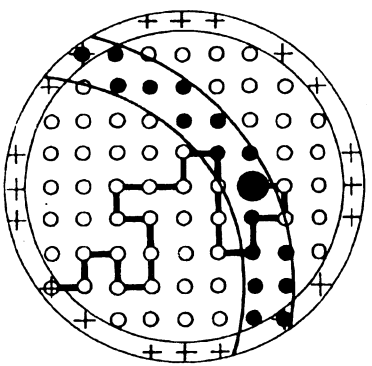

FIG. 3

A principle of calculation of the distribution of tethered-to-free end distances, $\rho_{TF}(r_{TF})$. + lattice sites in the surface area (where the tethered end of a chain may be located); ○ lattice sites inside the spherical core; ● lattice sites within a segmental spherical layer of the thickness d and the inner radius $r_i = i\,d$ (i.e., in the distance r_i from the tethered end), where the free end of the particular chain is located

The function $\rho_{TF}(r_{TF})$ does not depend directly on N as it is an average characteristics of a single chain. It should depend on the chain length, L. The results of calculations for higher densities show, however, that it does not depend significantly on L, either. The dependence on L is: (i) direct dependence on (Ll/R) which is almost hidden in our calculations for R = const, and (ii) indirect dependence on the segment density. In a restricted volume at high densities of occupied lattice sites, possible chain conformations are significantly pre-determined by the fraction of free lattice positions. Short parts of polymer chains behave as stiff subchains at the tetrahedral lattice (they are much more rigid than subchains at the simple cubic lattice) and therefore any decrease in the number of free positions is very important. The magnitudes of $\rho_{TF}(r_{TF})$ are therefore indirectly, but considerably affected by the term (NL/S_{tot}) – see Fig. 4*a*. Calculated distributions are quite flat with broad maxima in the region $r \in (4\,l, 8\,l)$. It follows from a comparison of $g_F(r)$ and $\rho_{TF}(r_{TF})$ that at higher segment densities, there is no "excluded dead" zone for the location of the free ends of chains close to the core surface. Non-zero values of $g_F(r \to 10\,l)$, $\rho_{TF}(r_{TF} \to 0)$ and $\rho_{TF}(r_{TF} \to 20\,l)$ suggest that there exist backcoiled conformations with small r_{TF}, as well as relatively stretched conformations with $r_{TF} \to 20\,l = 2\,R$. It must be kept in mind, however, that the true fractions of chains with certain end-to-end separations are obtained by multiplying function $\rho_{TF}(r_{TF})$ by numbers of lattice sites in corresponding segmental spherical layers.

Results for low densities (where an effect of non-accessible lattice sites, occupied by other chains, is not decisive) show a strong effect of geometrical restrictions induced by the small spherical volume on chain conformations (Fig. 4*a*, curves *1* – *3*). Even in systems, where there are many free lattice positions for chain conformations, the calculated functions $\rho_{TF}(r_{TF})$ differ considerably from those of isolated chains. Shapes of these curves, which are gaussian with maxima at $r_{TF} = 0$ for isolated long and flexible

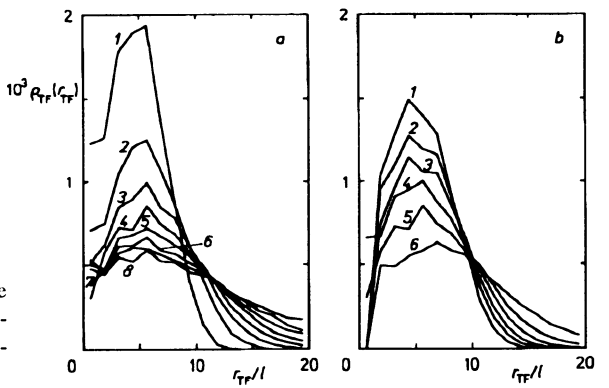

FIG. 4
Distribution of the tethered-to-free end distances, $\rho_{TF}(r_{TF})$, of individual chains for the same combinations of N and L as in Fig. 1

chains under under the ϑ-conditions, show the pronounced maxima in the region of r_{TF} from 5 l to 10 l, depending on L. Maxima are more pronounced for shorter chains which is in part a trivial consequence of the stiffness of short chains on the tetrahedral lattice, however.

The function, $\rho_{TF}(r_{TF})$ shows the slowest convergency from all calculated distributions and it is why it was used to test the quality of our calculations. The slow convergency is due in part to its physical meaning and to the way how it is calculated. Low absolute values of this function (which are a consequence of a large number of possible lattice positions where the free end of any chain may be located) worsen the statistics of the numbers of unprobable conformations. As functions $\rho_{TF}(r_{TF})$ are relatively flat, the predominating factor for the numbers of conformations with a certain value r_{TF} are the numbers of lattice sites in segmental layers which are used in calculations. These are extremely low for small r_{TF} and the statistics is therefore bad for $r_{TF} \to 0$ and the resulting values of $\rho_{TF}(r_{TF})$ are affected by large random errors. A small increase in some calculated values for $r_{TF} < l$ is not realistic from physical point of view, nevertheless the values for $r_{TF} > l$ are reasonable and quite accurate (see Appendix).

The three following functions concern distributions of the centers of gravity of chains in the core. The first one, $g_C(r)$, is simply the density of gravity centers of individual chains as a function of the distance from the core center, r. Its magnitude is controlled by the term N/S_{tot}. The distribution $g_C(r)$ is quite sharp for short chains and much broader with non-negligible values in the central region for longer chains (Fig. 5). This function alone does not tell much on the arrangement of individual chains, however a comparison with the two remaining distributions is quite useful.

Distributions of the distances of gravity centers of individual chains from either the tethered end, $\rho_{TC}(r_{TC})$, or the free end, $\rho_{FC}(r_{FC})$, are calculated similarly to the end-to-end distribution, $\rho_{TF}(r_{TF})$ and are defined for r_{TC}, respectively r_{FC} in the region $\langle 0, 2R \rangle$.

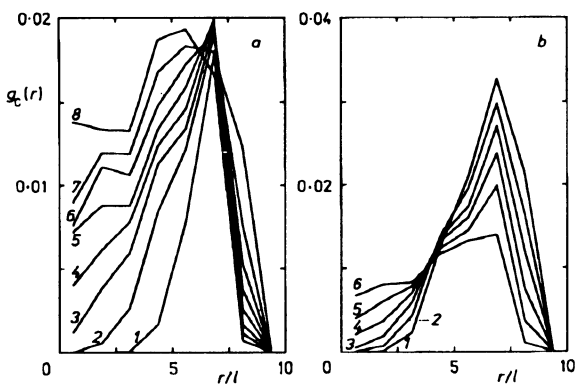

FIG. 5
Density of gravity centers of chains in the spherical core, $g_C(r)$, as a function of the distance from the center, r/l, for the same combinations of N and L as in Fig. 1

A comparison of $\rho_{TC}(r_{TC})$, $\rho_{FC}(r_{FC})$ and $g_C(r)$ gives information on an average stretching and orientation of the "tethered half" of the chain and the "free half" of the chain. Distributions of gravity centers, $g_C(r)$, $\rho_{TC}(r_{TC})$ and $\rho_{FC}(r_{FC})$ are shown in Figs 5, 6 and 7.

The comparison of $\rho_{TC}(r_{TC})$ and $\rho_{FC}(r_{FC})$ is very interesting and it shows that the "free halves" of chains are more coiled than the "tethered halves". Function $\rho_{FC}(r_{FC})$ is qualitatively similar to that for an isolated single chain with the maximum

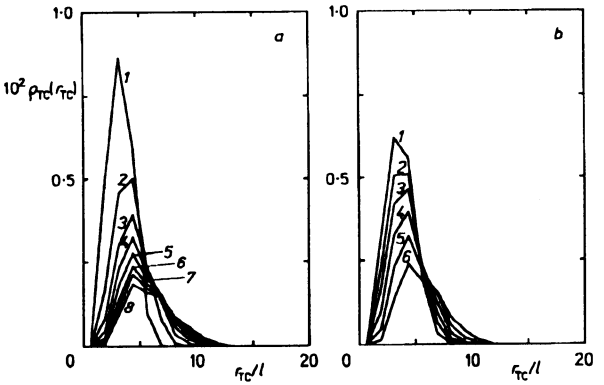

FIG. 6
Distribution of the tethered end-to-gravity center distances, $\rho_{TC}(r_{TC})$, of individual chains for the same combinations of N and L as in Fig. 1

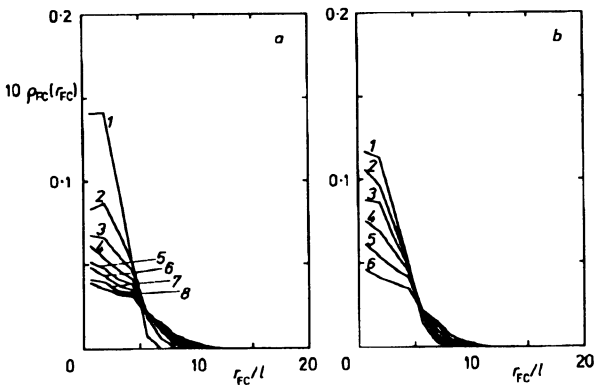

FIG. 7
Distribution of the free end-to-gravity center distances, $\rho_{FC}(r_{FC})$, of individual chains for the same combinations of N and L in Fig. 1

at $r_{FC} = 0$, whereas $\rho_{TC}(r_{TC})$ has quite a different shape with zero value at $r_{TC} = 0$, a maximum close to 5 *l* and a pronounced tailing reaching up to 12 – 14 *l*.

A comparison of maxima positions $(r_C)_m$ and $(r_{TC})_m$ in the functions $g_C(r)$ and $\rho_{TC}(r_{TC})$, respectively, suggests than an average orientation of the "tethered half" of the chain (i.e. the projection of r_{TC}), although not completely radial, does not decline considerably from the radial direction: values $[R - (r_C)_m]$ do not differ much from $(r_{TC})_m$.

The last function, which we have calculated in the course of our simulations, the distribution of the distances of the free ends of various chains from each other, $\rho_{FF}(r_{FF})$, is a function of an enormous importance for interpretation, or simulations of the excitation energy migration in micellar cores. The function $\rho_{FF}(r_{FF})$ is a normalized distribution which compares the actual numbers of individual pairs of free chain ends separated by increasing values of $r_{FF} \in \langle 0, 2R \rangle$, with numbers of all corresponding pairs of lattice sites for the same values of r_{FF}. A constant value of $\rho_{FF}(r_{FF})$, independent, of r_{FF} would mean a random distribution of r_{FF} distances. Figure 8 shows that the distribution of free end distances from each other is not completely random. An important conclusion for interpretation of excitation energy migration measurements is that the fraction of closely located pairs is lower than that in a random arrangement. Distribution of the free end-to-free end distances is more uniform for small numbers of long chains ($L > N$, Fig. 8*a*, curves *6*, *7* and *8*) which is a result of both a strong restrictive orientational effect of a small spherical volume on the coiling of long chains and their possible orientations, and an increased flexibility of long chains as compared with the short ones.

Results of calculations for larger spherical volumes, higher densities, lattices with a higher coordination number, which allow an increased flexibility of chains, a detailed comparison of structural characteristics obtained with various lattices and with those of an isolated chain, effect of interaction parameters, calculations for mixed systems con-

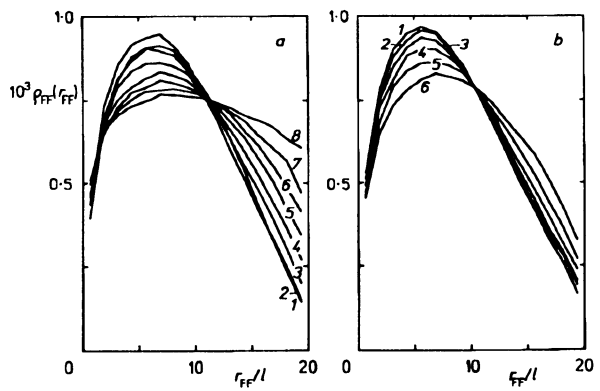

FIG. 8
Distribution of the distances of the free end of various chains, $\rho_{FF}(r_{FF})$, in the spherical core for the same combinations of N and L as in Fig. 1

taining two types of chains differing significantly in chain length, etc., will be presented in subsequent papers of this series.

CONCLUSIONS

a) Results of Monte Carlo simulations of tethered chain conformations in a restricted volume show a significant effect of geometrical restrictions on chain arrangements. Various structural and conformational characteristics of chains depend both on the number of chains, N, and the chain lengths (number of segments), L, and particularly on the average density, i.e. on the (NL).

b) Calculations for sufficiently long chains ($Ll > R$) at high densities ($\langle g_S \rangle > 0.5$) are suitable for simulations of swollen insoluble cores of multimolecular polymeric micelles.

c) Average conformations of the "tethered halves" and "free halves" of chains differ considerably from each other and the spatial distribution of the free ends within a sphere is not fully random.

APPENDIX

It is essential for any Monte Carlo calculation to be sure that the resulting data are the real ensemble average characteristics of an thermally equilibrated system. Practically it means that several conditions must be met, such as: (i) detailed balance, (ii) microscopic reversibility, etc. and a condition that the sampling succession is (iii) ergodic and (iv) long enough to reach the true thermal equilibrium. The fulfillment of requirements (i) to (iii) has been proven generally by Siepmann and Fren-

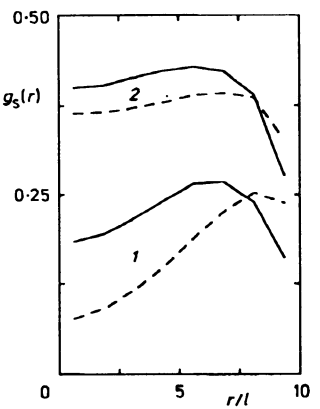

FIG. 9
A comparison of functions $g_S(r)$: *1* for $N = 20$, $L = 30$, and *2* $N = 20$, $L = 50$, calculated without (dashed curves) and with (full curves) the "thermal equilibration". The dashed curves represent results of $M \approx 10^4$ simultaneous arrangements of N chains within a spherical core (obtained by a simple self-avoiding walk). The full curves represent results of $M = 2 \cdot 10^3$ equilibrated arrangements of N chains (each of them was equilibrated N^2 times)

kel[18] for the sampling scheme, the modification of which we have employed in our calculations.

However, it is instructive to show an effect of the equilibration procedure that we used (steps *e*) and *f*) in Method). Figure 9 shows a comparison of functions $g_S(r)$, for systems with $N = 20$, $L = 30$, and $N = 20$, $L = 50$, calculated with equilibration (full curves), and without equilibration (dashed curves).

The effect of the number of generated micelles on the data (convergency of our sampling scheme) is shown in Fig. 10, where distributions $\rho_{FT}(r_{FT})$ for several values of generated micelles, M, are compared. Since one averaged micelle is a system containing usually more than 10^3 segments, and this system was equilibrated ca 10^3 times, the convergency on the M-scale is fairly fast (except for values for small r_{FT}).

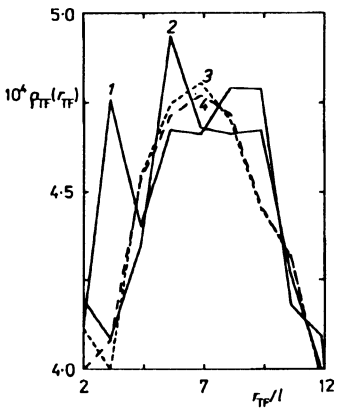

FIG. 10
A convergency of simulated data. A comparison of functions $\rho_{TF}(r_{TF})$, $N = 20$ and $L = 50$, for increasing numbers M of simulated equilibrated spherical cores: *1* $M = 200$, *2* $M = 600$, *3* $M = 4\,000$, *4* $M = 8\,000$. Due to an extensive equilibration of each core, even the curves for low M show a physically reasonable shape

The authors are obliged to Prof. P. Munk from the University of Texas at Austin, Tx., U.S.A., for very helpful discussions and suggestions, and to the Ministry of Education of the Czech Republic for financial support of this work (Grant No. FDR 0145).

REFERENCES

1. Tuzar Z., Kratochvíl P. in: *Surface and Colloid Science* (E. Matijevic, Ed.), Vol. 15, p. 1. Plenum Press, New York 1993.
2. Ellias H.-G., Bareiss R.: Chimia *21*, 53 (1967).
3. de Gennes P. G. in: *Solid State Physics* (J. Liebert, Ed.), Suppl. 14, p. 1. Academic Press, New York 1978; de Gennes P. G.: *Scaling Concepts in Polymer Physics*. Cornell University, Ithaca 1979.

4. Leibler L., Orland H., Wheeler J. C.: J. Chem. Phys. *79*, 3550 (1983).
5. Noolandi J., Hong M. H.: Macromolecules *16*, 1443 (1983).
6. Whitmore D., Noolandi J.: Macromolecules *18*, 657 (1985).
7. Meier D. J.: J. Polym. Sci., C *26*, 81 (1969).
8. Helfland E., Tagami Y.: J. Polym. Sci., B *9*, 741 (1971).
9. Helfland E., Sapse A. M.: J. Chem. Phys. *62*, 1327 (1975).
10. Nagarajan R., Ganesh K.: J. Chem. Phys. *90*, 5843 (1989).
11. ten Brinke G., Hadziioannou G.: Macromolecules *20*, 486 (1987).
12. Halperin A.: Macromolecules *20*, 2943 (1987).
13. Yuan X.-F., Masters A. J., Price C.: Polymer, in press.
14. Kremer K., Binder K.: Comp. Phys. Rep. *7*, 259 (1988).
15. Allen M. P., Tildesley D. J.: *Computer Simulations of Liquids*. Clarendon Press, London 1986.
16. Geyler S., Pakula T., Reitter J.: J. Chem. Phys. *92*, 2676 (1990).
17. Reitter J., Edling T., Pakula T.: J. Chem. Phys. *93*, 837 (1993).
18. Siepmann J. I., Frenkel D.: Mol. Phys. *75*, 59 (1992).
19. Wittmer J., Paul W., Binder K.: Macromolecules *25*, 6214 (1992).
20. Cifra P., Carasz F. E., MacKnight W. J.: Macromolecules *25*, 4895 (1992).
21. Kremer W., Grest G. S.: J. Chem. Soc., Faraday Trans., in press.
22. Rigby D., Roe R. J.: Macromolecules *23*, 5312 (1990).
23. Winkler R. G., Ludovice P. J., Yoon D. Y., Morawetz H.: J. Chem. Phys. *95*, 4709 (1991).
24. Li. Y., Mattice W. L.: Macromolecules *25*, 4942 (1992).
25. Berker A., Chynoweth S., Klomp V. C., Michopoulos Y.: J. Chem. Soc., Faraday Trans. *88*, 1719 (1992).
26. Rodriques K., Mattice W. L.: Polym. Bull. *25*, 239 (1991).
27. Rodriques K., Mattice W. L.: J. Chem. Phys. *94*, 761 (1991).
28. Rodriques K., Mattice W. L.: Langmuir *8*, 456 (1992).
29. Wang Y., Mattice W. L., Napper D. H.: Macromolecules *25*, 4073 (1992).
30. Wang Y., Mattice W. L., Napper D. H.: Langmuir *9*, 66 (1993).
31. Kron A. K., Pitsin O. P., Skvortsov A. M., Fedorov A. K.: Mol. Biol. *1*, 487 (1967).
32. Verdier P. H., Stockmayer W. H.: J. Chem. Phys. *36*, 227 (1962).
33. Metropolis N., Rosenbluth A. W., Rosenbluth M. N., Teller A., Teller H.: J. Chem. Phys. *21*, 1087 (1953).
34. van der Ploeg P., Berendsen H. J. C.: Mol. Phys. *49*, 233 (1983).
35. Haile J. M., O'Connel J. P.: J. Phys. Chem. *88*, 6363 (1984).
36. Jönsson B., Edholm O., Teleman O. J.: J. Chem. Phys. *85*, 2259 (1986).
37. Watanabe K., Klein M. L.: J. Phys. Chem. *93*, 6897 (1989).
38. Smit B., Seling K. S., Hilbers P. A. J., van Os N. M., Rupert L. A. M., Szleifer I.: Langmuir *9*, 9 (1993).
39. Murat M., Grest G. S.: Macromolecules *22*, 4054 (1989).
40. Chakrabarti A., Toral R.: Macromolecules *23*, 2016 (1990).
41. Murat M., Grest G. S.: Macromolecules *24*, 704 (1991).
42. Semenov A. N.: Sov. Phys. JETP, *61*, 733 (1985).
43. Procházka K., Kiserow D., Ramireddy C., Tuzar Z., Munk P., Webber S. E.: Macromolecules *25*, 454 (1992).
44. Kiserow D., Procházka K., Ramireddy C., Tuzar Z., Munk P., Webber S. E.: Macromolecules *25*, 461 (1992).

45. Procházka K., Kiserow D., Webber S. E., Ramireddy C., Munk P., Tuzar Z.: *Proceedings of the 34th IUPAC International Symposium on Macromolecules, Prague 1992*, 2-P92. Institute of Macromolecular Chemistry, Praha 1992.
46. Wang Z., Holden D. A., McCourt F. R. W.: Macromolecules *24*, 893 (1991).
47. Byers J. D., Parsons W. S., Webber S. E.: Macromolecules *25*, 5935 (1992).
48. Rosenbluth M. N., Rosenbluth A. W.: J. Chem. Phys. *23*, 356 (1955).
49. Cheng P.-L., Berney C. V., Cohen R. E.: Macromolecules *21*, 3442 (1988).

Translated by the author (K. P.).